JOURNAL OF COMPUTATIONAL PHYSICS **106**, 139–146 (1993)

A Quasi-Riemannian Method for the Solution of One-Dimensional Shallow Water Flow

A. PRIESTLEY*

Institute of Computational Fluid Dynamics, University of Reading, P.O. Box 220, Whiteknights, Reading RG6 2AX, United Kingdom

Received July 9, 1990

In this paper we consider the flow in an open channel, where supercritical flow may be induced by the geometry of the channel. The scheme presented calculates the Riemann invariants along characteristic curves and hence has no CFL limit. The presence of source terms may lead to a restriction on the time-step though, to ensure the stability of the ODE solver used. A high order monotone interpolation is used to provide accuracy whilst not inducing oscillations at hydraulic jumps.

1. INTRODUCTION

The Preissman scheme, Preissman [8], has long been a favourite of hydraulic engineers. It is simple, accurate, and owing to its implicitness, large time-steps can be taken. However, it does not perform well at discontinuities in the solution. Flux limited schemes, for example Roe's scheme, Roe [14], perform well at shocks but not necessarily in the presence of source terms; see Sweby [18] for a discussion of this point. Roe's scheme is not cheap. It relies upon a characteristic decomposition and upwinding. Second-order forms require even more logical switching. Whilst this expense can be justified in situations where there are jumps in the solution, it seems rather inefficient for entirely smooth flows.

In this paper we present a method that is efficient when the flow is smooth and yet can give monotone solutions even at shocks.

2. THE ST. VENANT EQUATIONS AND THE QUASI-RIEMANNIAN SCHEME

The St. Venant equations, see Chow [3] for example, for rough-turbulent flow in an open channel are

$$\frac{\partial A}{\partial t}+\frac{\partial Q}{\partial x}=0 \tag{1a}$$

$$\frac{\partial Q}{\partial t}+\frac{\partial}{\partial x}\left(\frac{Q^2}{A}\right)+gA\left[\frac{\partial h}{\partial x}+\frac{Q\,|Q|}{K^2}\right]=0, \tag{1b}$$

where

A = cross-sectional area = breadth × depth = $B \times d$ (only rectangular channels are considered here)

Q = massflow

g = acceleration due to gravity

h = height of free surface = $d+z$, where z is the height of the river bed

$Q\,|Q|/K^2$ is the friction term chosen to give the fully rough-turbulent form in this case

$K = A/M$ (hydraulic radius)$^{2/3}$, where the hydraulic radius = A/wetted perimeter, M is Manning's constant for which we take a value of 0.03. For rectangular channels, wetted perimeter = $2d+B$.

Also, for future reference,

β = bed-slope = $\partial z/\partial x$

c = wave-speed = $(gA/B)^{1/2}$.

u = velocity.

$|u|/c$ = the Froude number.

To apply our chosen scheme we need to rewrite Eq. (1). Equation (1b) is put in terms of the velocity u and Eq. (1a) in terms of the wave speed c. The St. Venant equations become

$$u_t+uu_x+2cc_x=g\left(-\frac{Q\,|Q|}{K^2}-\beta\right) \tag{2a}$$

$$c_t+\frac{cu_x}{2}+uc_x=-\frac{ucB_x}{2B}. \tag{2b}$$

* The work reported here forms part of the research programme of the Reading/Oxford Institute for Computational Fluid Dynamics and has been supported by the S.E.R.C. under Grant Number GR/E72256.

0021-9991/93 $5.00

We then write Eq. (2) in the form

$$\mathbf{u}_t + E\mathbf{u}_x = \mathbf{b},$$

where

$$\mathbf{u} = \begin{pmatrix} u \\ c \end{pmatrix}$$

$$E = \begin{pmatrix} u & 2c \\ c/2 & u \end{pmatrix}$$

$$\mathbf{b} = \begin{pmatrix} g\left(-\dfrac{Q|Q|}{k^2} - \beta\right) \\ -\dfrac{ucB_x}{2B} \end{pmatrix}.$$

The eigenvalues of E are

$$\lambda^+ = u + c$$

$$\lambda^- = u - c.$$

The associated eigenvectors are then

$$\mathbf{e}^- = (2, -1)^T \quad \text{and} \quad \mathbf{e}^+ = (2, 1)^T.$$

Defining the matrix H to be given by $[\mathbf{e}^-, \mathbf{e}^+]$ we obtain

$$H = \begin{pmatrix} 2 & 2 \\ -1 & 1 \end{pmatrix}$$

and the new vector

$$\mathbf{v} = H^{-1}\mathbf{u}.$$

We now have

$$\mathbf{v}_t + H^{-1}EH\mathbf{v}_x = H^{-1}\mathbf{b}.$$

Expanded, this becomes, putting $F^+ = u + 2c$ and $F^- = u - 2c$,

$$F_t^+ + \lambda^+ F_x^+ = g\left(-\frac{Q|Q|}{K^2} - \beta\right) - \frac{ucB_x}{B}$$

$$F_t^- + \lambda^- F_x^- = g\left(-\frac{Q|Q|}{K^2} - \beta\right) + \frac{ucB_x}{B}.$$

Equations (1) can now be rewritten as

$$\frac{d^+F^+}{dt} = b^1 \tag{3a}$$

$$\frac{d^-F^-}{dt} = b^2 \tag{3b}$$

with

$$\frac{d^\pm}{dt} = \frac{\partial}{\partial t} + \lambda^\pm \frac{\partial}{\partial x}.$$

Equations (3) are now in a form suitable for applying a Lagrangian type scheme to. Perhaps, though, we should call this a Riemannian scheme to avoid confusion with schemes that use the fluid velocity u, as is normally the case with Lagrangian methods.

The use of the Riemann invariants has been suggested before by Goussebaile and Lepeintre [5]. However, we believe that our method is better suited to the present problems for a number of reasons, stemming from the way that the Lagrangian/Riemannian derivatives are treated.

In Goussebaile and Lepeintre a finite element method is used for the advection step introduced in Benqué *et al.* [2]. (See also Morton, Priestley, and Süli [7] for a discussion of this and related schemes.) Being essentially a least squares fit, this Lagrangian method suffers from oscillations at shocks. Therefore a flux-limited scheme had to be used with the predicted values from the Riemannian step to keep monotonicity. Although the flux-limited scheme undoubtedly benefits from the use of these predicted upwinded values it seems rather inefficient, even more so since the flux-limited step imposes a CFL restriction of one on the method, whereas the Riemannian part of the scheme would have no such limit.

Here we suggest a scheme that is Riemannian and monotone. In the meteorological literature it is called the semi- or quasi-Lagrangian method. See Robert [12, 13], Bates [1], Staniforth and Temperton [16], Ritchie [11], and Temperton and Ritchie [19] for a flavour of this work.

We solve Eq. (3) and the trajectory problems

$$\frac{dX^\pm}{dt} = \lambda^\pm \tag{4}$$

with initial data $x(\Delta t) = x_i \forall i$, backwards in time, by any ODE method we choose. Here, for simplicity, we will use the forward Euler's method for the time derivative. The results that we will be presenting are actually for steady-state problems, so a time-accurate solution to Eqs. (3) and (4) is not of paramount interest. For problems that are truly transient in nature we might expect to have to use higher order ODE solvers. See Staniforth and Côté [15] for an example of the use of the mid-point rule and Temperton and Staniforth [20] and McDonald and Bates [6] for other schemes.

We will now denote $F^\pm$, $\lambda^\pm$, and $b^\pm$ by the generic quantities F, λ, and b; i.e., the steps outlined below for λ, for example, will need repeating for both the λ^+ characteristic and the λ^- characteristic.

Suppose we require the value of $F_{i+\frac{1}{2}}^{n+1}$. The characteristic

curve is traced back to the old time-level. In a two time-level scheme this involves the calculation of the point $X_{i+2}(0)$, where we have added the subscript $i+2$ to denote the starting point for this trajectory. Using Euler's method, corresponding to a straightline approximation to the characteristic curve, this is then given by

$$X_{i+2}(0) = x_{i+2} - \Delta t\, \lambda^n(x_{i+2});$$

see Fig. 1.

We now know that from Eq. (3),

$$F^{n+1}_{i+2} = F^n(X_{i+2}(0)) + \Delta t\, b^n(X_{i+2}(0)),$$

again using Euler's method to solve the ODE. Again we stress that Euler's method has been chosen for simplicity and to give an explicit scheme, and we are in no way forced to use this method in our scheme. We can then compute $F^n(X_{i+2}(0))$ by interpolation from the neighbouring points F^n_{i-1}, F^n_i, F^n_{i+1}, etc. A cubic interpolation is chosen to provide accuracy but we also require the cubic polynomial to be monotone to avoid problems at large gradients. This question has been addressed by Fritsch and Carlson [4].

Consider a cubic polynomial function $p(x)$ on the interval $[x_i, x_{i+1}]$ such that $p(x)$ is monotone and

$$p(x_i) = F_i$$
$$p(x_{i+1}) = F_{i+1}.$$

We can write $p(x)$ on each sub-interval in terms of the cubic Hermite basis functions to obtain

$$p(x) = F_i H_1(x) + F_{i+1} H_2(x) + d_i H_3(x) + d_{i+1} H_4(x),$$

where

$$d_j = p'(x_j), \qquad j = i, i+1,$$
$$H_1(x) = \phi((x_{i+1} - x)/h_i),$$
$$H_2(x) = \phi((x - x_i)/h_i),$$
$$H_3(x) = -h_i \psi((x_{i+1} - x)/h_i),$$
$$H_4(x) = h_i \psi((x - x_i)/h_i),$$

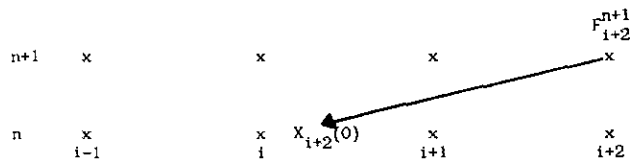

FIG. 1. Interpolation point found by following an approximation to the characteristic path back.

with

$$h_i = x_{i+1} - x_i,$$
$$\phi(t) = 3t^2 - 2t^3,$$
$$\psi(t) = t^3 - t^2.$$

Letting $\Delta_i = (F_{i+1} - F_i)/h_i$ we can rewrite the Hermite cubic polynomial as

$$p(x) = \left[\frac{d_i + d_{i+1} - 2\Delta_i}{h_i^2}\right](x - x_i)^3 + \left[\frac{-2d_i - d_{i+1} + 3\Delta_i}{h_i}\right](x - x_i)^2 + d_i(x - x_i) + F_i. \tag{5}$$

As it stands (5) will not be monotone in general. Monotonicity is ensured by limiting the values of d_i and d_{i+1}, cf. Sweby [17].

An obvious necessary condition for monotonicity is that

$$\text{sign}(d_i) = \text{sign}(d_{i+1}) = \text{sign}(\Delta_i). \tag{6}$$

Writing $\alpha = d_i/\Delta_i$ and $\beta = d_{i+1}/\Delta_i$, $\Delta_i \neq 0$, Fritsch and Carlson [4] were able to prove that (5) is always monotone if and only if (6) holds in conjection with one or both of the conditions on (α, β),

$$0 \leqslant \alpha \leqslant 3, \qquad 0 \leqslant \beta \leqslant 3 \tag{7a}$$

and

$$\phi(\alpha, \beta) \leqslant 0, \tag{7b}$$

where

$$\phi(\alpha, \beta) = (\alpha - 1)^2 + (\alpha - 1)(\beta - 1) + (\beta - 1)^2 - 3(\alpha + \beta - 2).$$

For obvious reasons (7a) is the more usually applied constraint.

This still leaves us with the question of how to choose the estimates of the derivatives. Rasch and Williamson [10] have performed an excellent series of tests on the choices of derivative and on the type of polynomial. In their tests the Hyman derivative

$$d_i = \frac{-\Delta_{i-2} + 7\Delta_{i-1} + 7\Delta_i - \Delta_{i+1}}{12}$$

performed consistently well in relation to the monotonic cubic polynomial.

The derivative that we will use here was first described by Priestley [9] and is given by

$$d_i = \frac{-3\Delta_{i-2} + 19\Delta_{i-1} + 19\Delta_i - 3\Delta_{i+1}}{32}.$$

This has the same computational cost as the Hyman derivative estimate but it was found that for constant coefficient advection the estimate given above consistently gave better results, although the improvement was only marginal.

3. THE PROBLEM AND THE RESULTS

We consider flow in a rectangular channel only. This is not a restriction on the scheme, which can equally well be applied to non-rectangular channels or pipes. Three flow regimes are considered. Entirely sub-critical, entirely super-critical, and sub-critical → super-critical → sub-critical. These results all reach a steady state, but the evolutionary form of the equations is always used as described previously.

The boundary conditions are applied by supplying values for characteristic curves that leave, where by leave we mean that as we track them backwards in time they leave the domain. In sub-critical flow the F^+ characteristic curve will leave the domain at the upstream end and the F^- characteristic at the downstream end. Hence, if we wish to impose a value for the massflow at the upstream, inflow, boundary we must give a value to F^+ here such that the required value of Q is then obtained. (The value of F^- at this point can still be found by interpolation from the interior.) At the downstream end it is the F^- Riemann invariant that we need to supply a value for. Here we applied a zero curvature boundary condition, i.e., $d_{xx} = 0$ at outflow. This boundary condition is somewhat arbitrary. In practice it is likely that depth itself will be specified at outflow but in these test problems there is no such information and trying to fix depth, or F^-, does not give such smooth solutions at outflow as the zero curvature condition. Values for F^- are then supplied for the λ^- characteristics that leave the domain to enforce this condition.

In the case of super-critical flow, no characteristics leave the domain at the outflow end and so no boundary conditions are needed there. At inflow both the λ^+ and λ^- characteristics leave the domain and so values of F^+ and F^- are provided that fix the massflow and the boundary condition on depth.

The parameters available to us in choosing the channel are its breadth and slope. Here the channel is 10,000 m long and has a smooth constriction that goes from a breadth of 10 m → 5 m → 10 m, see Fig. 2.

The bed-slope is taken to be a constant value except between 4500 and 5500 m, where twice this value is taken. See Fig. 3 for a typical cross section. The massflow is

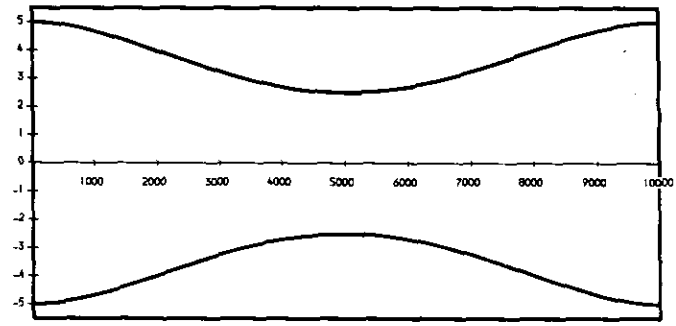

FIG. 2. Smoothly constricted channel.

enforced to be $20\,m^3\,s^{-1}$ at inflow and this is the value taken for the initial data. A uniform depth of 2 m is taken to start the calculation.

At steady state, as we can easily see from Eq. (1a), the massflow should be a constant everywhere, equal to the value imposed at inflow. We will use this fact to give a guide to the accuracy of our scheme. Three quantities will be measured, as described below, where we denote the number of points by npt;

(1) A discrete l_2 error given by

$$\sqrt{\Delta x \sum_{i=1}^{npt} (Q_i - Q_{exact})^2},$$

(2) The relative percentage error in conservation of massflow given by

$$100\left(\sum_{i=1}^{npt} (Q_i - Q_{exact})\right) \Big/ \sum_{i}^{npt} Q_{exact},$$

where a minus sign then means a loss in total massflow.

(3) The relative percentage error in massflow at outflow $= 100(Q_{npt} - Q_{exact})/Q_{exact}$.

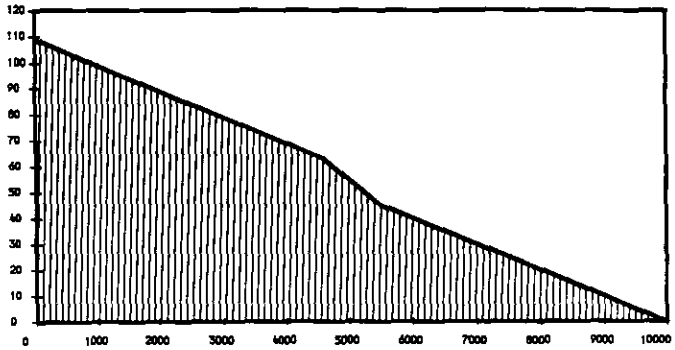

FIG. 3. Typical cross section of river.

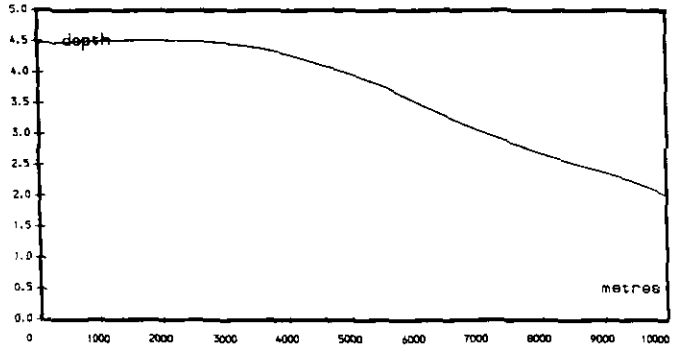

FIG. 4. Depth with bed-slope of 1/10000.

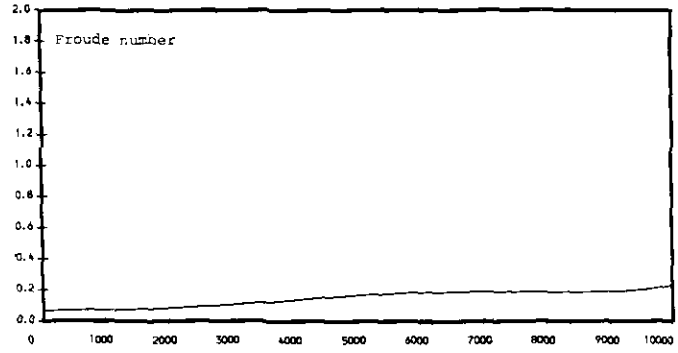

FIG. 6. Froude number with bed-slope of 1/10000.

Depth, massflow, and Froude number have been plotted out for the following slopes:

$\frac{1}{10,000}$,	Figs. 4–6
$\frac{1}{1,000}$,	Figs. 7–9
$\frac{1}{500}$,	Figs. 10–12
$\frac{1}{100}$,	Figs. 13–15
$\frac{1}{50}$,	Figs. 16–18.

The results show that this Riemannian scheme copes well with both the smooth and discontinuous flows.

We now look more closely at two of the results, using different grids. Tables I–III refer to the case of the entirely sub-critical flow generated by the bed-slope of 1:10000. Tables IV and V relate to the trans-critical case given by a bed-slope of 1:100.

There are several things to note about these results. First, we point out that with the 80-s time-stepping on the 25-m grid for the 1:10000 river the maximum CFL is nearly 25. Having said this though, it is clear that the results get better with the smaller time-steps. Indeed, we have a near linear convergence in Δt, as we might expect with using Euler's method with the time stepping. To take full advantage of the

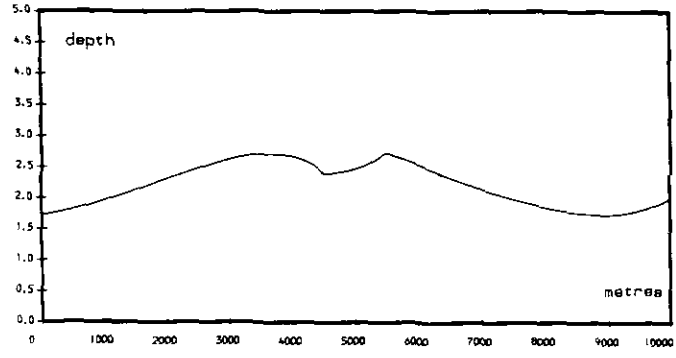

FIG. 7. Depth with bed-slope of 1/1000.

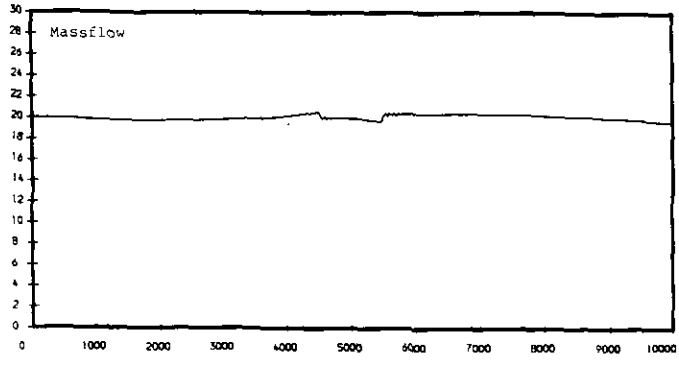

FIG. 8. Massflow with bed-slope of 1/10000.

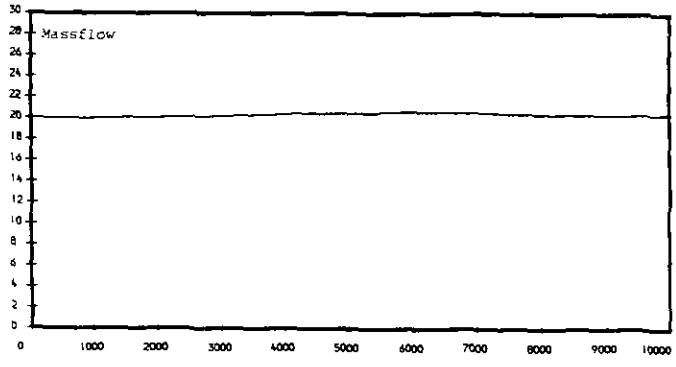

FIG. 5. Massflow with bed-slope of 1/10000.

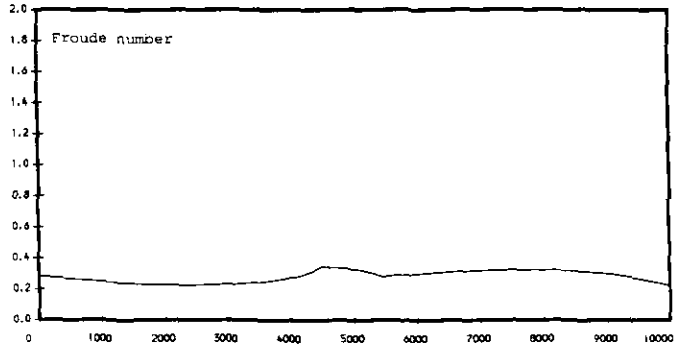

FIG. 9. Froude number with bed-slope of 1/1000.

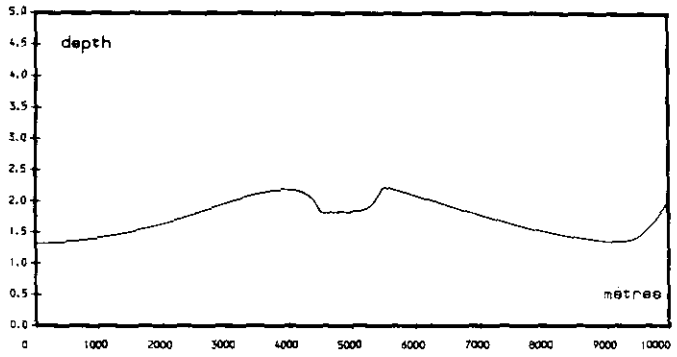

FIG. 10. Depth with bed-slope of 1/500.

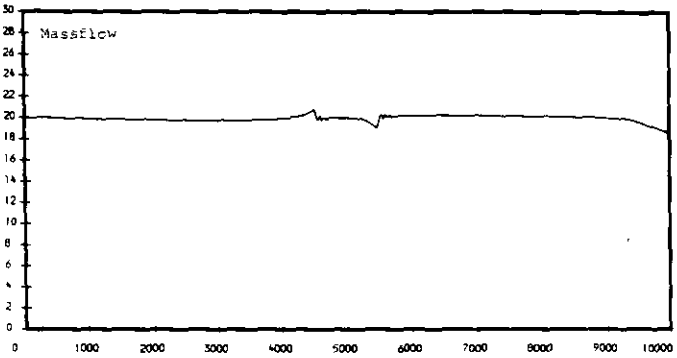

FIG. 11. Massflow with bed-slope of 1/500.

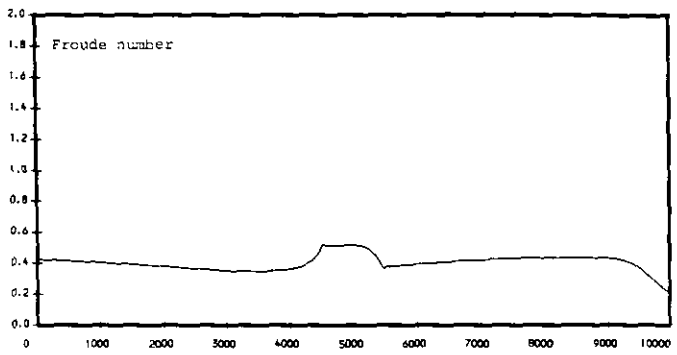

FIG. 12. Froude number with bed-slope of 1/500.

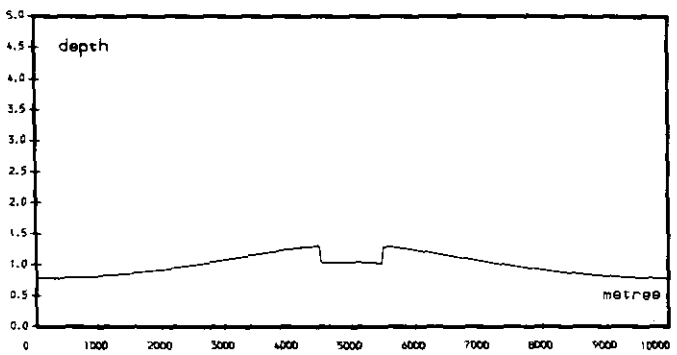

FIG. 13. Depth with bed-slope of 1/100.

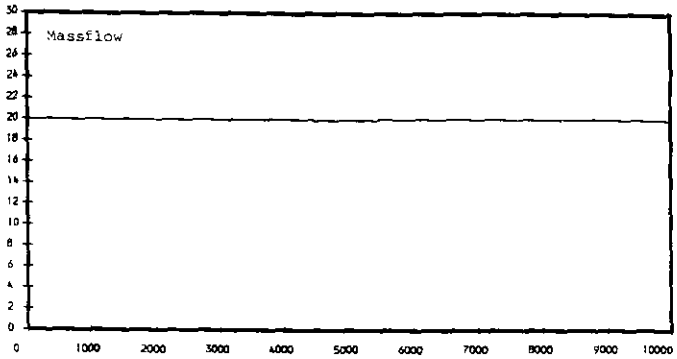

FIG. 14. Massflow with bed-slope of 1/100.

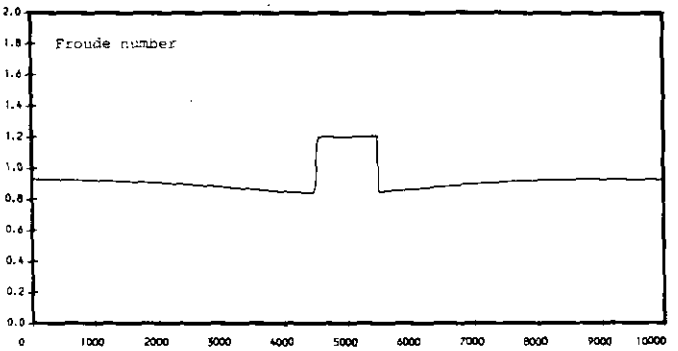

FIG. 15. Froude number with bed-slope of 1/100.

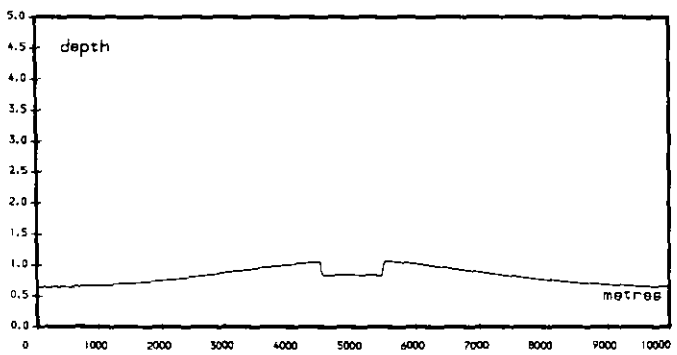

FIG. 16. Depth with bed-slope of 1/50.

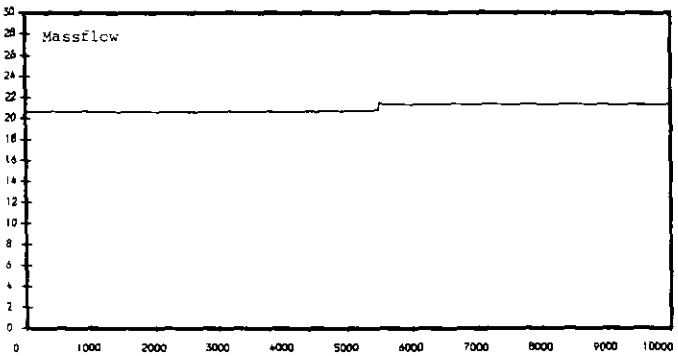

FIG. 17. Massflow with bed-slope of 1/50.

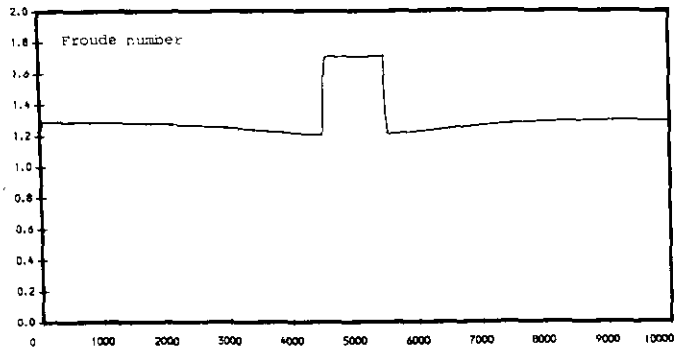

FIG. 18. Froude number with bed-slope of 1/50.

method we would have to consider other ODE solvers for the time-stepping.

Second, refining the grid had little or no effect on the quality of the results. Indeed, we were able to obtain visually identical results to those in Tables I–III on grids of 500 m or greater. These results would not converge to steady state though, with the residuals oscillating around values of $10^{-6} \rightarrow 10^{-7}$. All the results here converged to machine zero.

Finally, although much coarser special grids could be used, much greater values of Δt could not. In all of the above cases a re-doubling of Δt led to a violation of the stability limit of Euler's method for Eq. (3). This, again, could be overcome by a more sophisticated ODE solver if the time-step were felt to be too restrictive.

TABLE I

Errors for River Slope 1:10000 with $\Delta x = 100$ m

Δt	Percentage error in total massflow	Percentage error in outflow massflow	l_2 error in massflow
20 s	1.483	0.647	39.322
40 s	7.4	7.462	176.52
80 s	16.706	19.5805	407.18

TABLE II

Errors for River Slope 1:10000 with $\Delta x = 50$ m

Δt	Percentage error in total massflow	Percentage error in outflow massflow	l_2 error in massflow
10 s	0.292	1.843	13.076
20 s	3.4896	3.242	82.358
40 s	7.396	7.822	175.9
80 s	16.734	19.5775	406.48

TABLE III

Errors for River Slope 1:10000 with $\Delta x = 25$ m

Δt	Percentage error in total massflow	Percentage error in outflow massflow	l_2 error in massflow
10 s	1.696	1.514	39.823
20 s	3.483	3.459	82.068
40 s	7.407	7.5073	175.806
80 s	16.73	19.6165	405.64

TABLE IV

Errors for River Slope 1:100 with $\Delta x = 25$ m

Δt	Percentage error in total massflow	Percentage error in outflow massflow	l_2 error in massflow
10 s	0.258	−12.1385	63.195
20 s	−0.965	−15.0	165.452

TABLE V

Errors for River Slope 1:100 with $\Delta x = 12.5$ m

Δt	Percentage error in total massflow	Percentage error in outflow massflow	l_2 error in massflow
5 s	0.2096	−7.612	30.348
10 s	−0.1509	−16.5165	60.8020

4. CONCLUSION

We have introduced, or perhaps more accurately, brought together various ideas that result in a very accurate scheme that is explicit and yet can use large time-steps and is monotonic. This has been demonstrated on a number of test problems. The scheme can be used not only for river flow but also pipe flow and in gas dynamics. This is not a shock capturing scheme, but with the monotonic interpolation it is possible to extend the potential application of this method from entirely smooth flows to flows where discontinuities may be forced by the presence of weirs etc.

Here we just solved the ODEs for the Riemann invariants, Eq. (5), using Euler's method. This was perfectly adequate for demonstrating the method here but higher order time-stepping would certainly be needed to take full advantage of the stability of the scheme.

REFERENCES

1. J. R. Bates, *Lectures in Applied Mathematics*, Vol. 22 (Am. Math. Soc., Providence, RI, 1985), p. 1.
2. J. P. Benqué, G. Labadie, and J. Ronat, in *Proceedings, 4th int. Symp. on Finite Element Methods in Flow Problems*, edited by T. Kawai (North-Holland, Amsterdam/Oxford/New York, 1982), p. 295.
3. V. T. Chow, *Open-Channel Hydraulics* (McGraw–Hill, 1959), p. 525.
4. F. N. Fritsch and R. E. Carlson, *SIAM J. Numer. Anal.* **17**, No. 2 (1980).
5. J. Goussebaille and F. Lepeintre, in *Proceedings, Int. Conf. Bradford Sept. 1989, on Hydraulic and Environmental Modelling of Coastal, Estuarine and River Waters*, edited by R. A. Falconer, P. Goodwin, and R. G. S. Matthew (Gower Technical, England, 1989).
6. A. McDonald and J. R. Bates, *Mon. Weather. Rev.* **115**, 737 (1987).
7. K. W. Morton, A. Priestley, and E. E. Süli, *RAIRO Modél. Math. Anal. Numér.* **22**, No. 4, 625 (1988).
8. A. Preissman, in *First Congress of the French Association for Computation, Grenoble, France, 1961.*
9. A. Priestley, University of Reading Numerical Analysis Report 9/89, 1989 (unpublished).
10. P. M. Rasch and D. L. Williamson, *SIAM J. Sci. Stat. Comput.* **11**, No. 4 (1990).
11. H. Ritchie, *Mon. Weather Rev.* **115**, 608 (1987).
12. A. J. Robert, *Atmos-Ocean* **19**, 35 (1981).
13. A. J. Robert, *J. Meteorol. Soc. Jpn* **60**, 319 (1982).
14. P. L. Roe, *J. Comput. Phys.* **43** (1981).
15. A. Staniforth and J. Cote, in *Twelfth Int. Conf. on Numerical Methods in Fluid Dynamics, 1990*, edited by K. W. Morton, Lecture Notes in Physics, Vol. 371, (Springer-Verlag, New York/Berlin, 1990), p. 63.
16. A. Staniforth and C. Temperton, *Mon. Weather Rev.* **114**, 2078 (1986).
17. P. K. Sweby, *Lectures in Applied Mathematics*, Vol. 22 (Am. Math. Soc., Providence, RI, 1985), p. 289.
18. P. K. Sweby, in *Notes on Numerical Fluid Mechanics*, Vol. 24, edited by J. Ballmann and R. Jeltech (Vieweg, Brunswick, 1989), p. 599.
19. C. Temperton and H. Ritchie, in *ECMWF Workshop Proceedings on Techniques for Horizontal Discretization in Numerical Weather Prediction Models, November 2–4, 1987*, p. 47.
20. C. Temperton and A. Staniforth, *Q. J. R. Meteorol. Soc.* **113**, 1025 (1987).